STUDIES OF PPLO INFECTION

III. Electron Microscopic Study of Brain Lesions Caused by Mycoplasma Neurolyticum Toxin

By FERNANDO ALEU,* M.D., and LEWIS THOMAS, M.D.

(From the Departments of Neurology and Medicine, New York University School of Medicine, and the Laboratory of Neuropathology of the Office of the Chief Medical Examiner of New York City)

Plates 101 to 107

(Received for publication 27 June 1966)

Rolling disease, the acute encephalopathy produced by *Mycoplasma neurolyticum* toxin in rats and mice, was shown in the preceding paper (1) to be associated with brain lesions which, by light microscopy, appeared to consist of focal aggregates of large vacuoles in the cortex and white matter. Areas of demyelination were also observed. In animals surviving for longer than 2 days, extensive necrotizing lesions resembling ischemic necrosis were encountered.

In order to determine the nature and origin of the vacuoles, and the ultrastructural basis of the myelin injury, electron microscopic studies were undertaken with brain tissue from animals with rolling disease. Rats were used because of the relative abundance of white matter, and the greater ease of brain perfusion for electron microscopic study; animals surviving with neurological manifestations for 16 hr were studied since the vacuolar lesions seemed most prominent by light microscopy at this time.

Material and Methods

Fifteen Sprague-Dawley rats, weighing approximately 150 g, were used for this study. A dose of lyophilized toxin (1) was selected which caused obvious neurological disturbances (usually paralysis, clonic twitching of the extremities, and turning movements of the body), without killing all animals within the first few hours. With the lot of toxin used, this dose was 20 mg, contained in 1 ml distilled water, injected intravenously. All of the animals were still alive, although very ill, 16 hr after the injection. At this time, 10 were killed by perfusion through the ascending aorta with cold 3% glutaraldehyde solution in 0.1 M sodium phosphate. 30 ml of perfusate were administered, over a period of about 12 min. Samples of brain tissue were then removed and postfixed in osmium for 90 min. Five animals were anesthetized with pentobarbital, and biopsies of cortex and white matter were taken; these were immediately immersed in osmium tetroxide and also fixed for 90 min. Dehydration of both sets of tissue were carried out in graded acetones. Thirty blocks were obtained from each animal and em-

* Career Research Development Award United States Public Health Service IK3 NB 25 406-01.

bedded in Araldite (Ciba Co., Duxford, England). The blocks were sectioned on an LKB microtome with glass knives. The electron microscope was a Siemens Elmiskop I.

All blocks were examined by thick sections, and thin sections were prepared from pertinent areas.

RESULTS

The findings were essentially the same in all animals, with only minor variations in degree of abnormality.

Cortex

The general appearance of the neuropil was remarkable. There were numerous large, clear vacuolar spaces, measuring up to 40 μ in diameter (Figs. 1 to 3). The vacuoles were usually free of recognizable organelles, but some contained mitochondria and small aggregates of fibrillar material similar to structures found in fibrous astrocytes. A few vesicular profiles and granular densities were also noted.

The vacuoles were bounded by distended cytoplasmic membranes, apparently intact and well preserved. Occasionally, breaks in the membrane were encountered. The apposition of the membranes of adjacent vacuoles formed delicate filamentous septae. In places, vacuoles were separated from each other by narrow bands of relatively normal, compact neuropil, Fig. 2.

The vacuoles were interpreted as representing markedly swollen astrocytes. They were always bound by a double membrane, and were most prominent within the deep cortical layers and in the vicinity of blood vessels. The astrocytic nuclei ranged in appearance from essentially normal (Fig. 4) to extensively altered (Fig. 5). In some, the nucleoplasm consisted of unevenly distributed fine granular material; the nuclear membranes were often fragmented. There were usually 1 or 2 nucleoli. The cytoplasm contained many osmiophilic bodies with the appearance of lipofuscin, dispersed among vesicular structures resembling mitochondria, with scanty cristae within the clear matrix. There were also swollen sacs of endoplasmic reticulum, and occasional autophagic vacuoles containing poorly defined lamellar profiles (Fig. 5).

The neurons in the immediate vicinity of aggregates of vacuoles appeared normal in most instances. The nucleus, cytoplasmic organelles, and ribonucleoprotein particles were within normal limits.

Microglia.—A small number of cells were noted with lobular nuclei and rather dense cytoplasm, free from filaments and with little endoplasmic reticulum. The cytoplasm contained abundant lysosomes, mitochondria, and vacuoles. In a few instances they exhibited short blunt processes extending around myelin sheaths, suggesting early phagocytic activity. The cells were considered to be active microglial elements with the properties of histiocytes (Fig. 6).

Blood Vessels.—The astrocytic foot processes attached to the basement membranes of capillaries were enormously distended, forming membrane-bound

vacuolar spaces measuring as large as 50 μ across (Fig. 7). Because of these structures, the vessels often appeared to be "floating" in large, empty spaces. The vessels themselves were essentially normal in structure. The endothelial cells contained the usual number of vesicles measuring around 600 A, small amounts of rough endoplasmic reticulum, and few mitochondria and Golgi complexes. At the junction of neighboring endothelial cells the apposed membranes exhibited well formed 1000 A desmosomes close to the lumen side. The remaining endothelial junction consisted of the two almost parallel lines of adjacent cell membranes separated by a clear zone measuring 100 A (Fig. 8). The basement membrane of the capillaries was a well demarcated, faintly fibrillar band about 500 A in thickness, and in some areas surrounded the body of a pericyte.

White Matter

The myelinated axons were loosely arranged, often separated from each other by distended cellular processes similar to those in the cortex (Fig. 9) or by an increased extracellular compartment (Fig. 10). In many intances, these membrane-bound processes caused displacement and distortion of the shape of myelin sheaths (Figs. 12 and 13). A common occurrence was the presence of a large periaxonal space between the neural structure and its myelin wrapping, resulting in large, seemingly empty chambers (Fig. 11). In other areas, early degeneration of the myelin sheath with the formation of small digestion chambers surrounding an axon were seen (Fig. 14). The axons themselves appeared intact, with homogeneous axoplasm and the normal number of neurofibrils and mitochondria. No evidence of Wallerian degeneration was found. Occasionally, the myelin of an intact axon had irregular splits in its lamellae which involved both major and minor periods; these were considered to represent minor artifacts.

In many areas of the white matter, the vessels and myelin elements were separated from each other by apparently free, extracellular fluid, without recognizable limiting membranes. It could not be determined whether this fluid came directly from the vascular elements or through disrupted astrocytic vacuoles or from some other source.

A few oligodendroglial cells were seen in the white matter. Their nuclei and narrow cytoplasmic rim were of normal size and density. The cytoplasmic organelles were normal.

DISCUSSION

The principal and apparently basic ultrastructural lesion was the massive swelling of astrocytes and their processes throughout the brain. Although the present study was confined to the brains of rats obtained 16 hr after an injection of toxin, it should be noted that the same change has been seen in rats killed

6 hr after toxin, and in mice. The degree of intracellular edema was sufficient to cause distortion and compression of myelinated axons, and furnishes an adequate explanation for the extensive lesions of bilateral, symmetrical ischemic necrosis which were observed by light microscopy in animals surviving 2 days or longer (1).

The distribution of swollen astrocytes in patchy aggregates of large size, but not diffusely throughout the cortex, serves to differentiate this reaction from other varieties of cortical edema. The lesions are partially reminiscent of some encountered in a number of human degenerative brain diseases loosely grouped together under the designation of "spongiform encephalopathy," (2–4).

Although most of the abnormal accumulations of fluid were within astrocytes, or within membrane-bound processes arising from these cells, considerable amount of fluid was free in the extracellular space of the white matter. It is possible that this came from ruptured cells, but the question cannot be settled at this time. Further studies are planned for evaluation of the extracellular space of the brain by other techniques.

In the preceding paper evidence was presented which indicated that *M. neurolyticum* toxin acts by way of receptors contained within the vascular compartment of the brain (1). Conceivably, binding of the toxin to a receptor in the capillary basement membrane, or in the astrocytic podocytes, might alter permeability at this level and cause the entry of fluid into systems of astrocytes. Ultrastructural studies failed, however, to provide information concerning a physical basis for this change in the barrier. The capillaries, their basement membranes or the attached astrocytic membranes showed no evidence of endothelial gaps, such as those described by Majno (5), or other forms of damage. Further studies, utilizing ferritin and thorotrast as indicators of vascular integrity, are planned.

SUMMARY

The ultrastructure of the experimental encephalopathy caused by *Mycoplasma neurolyticum* toxin has been studied. The primary changes are (*a*) massive distention of astrocytes by fluid, associated with degenerative changes in these cells, (*b*) mechanical displacement and compression of myelinated axons by swollen astrocytic processes, (*c*) the appearance of free, extracellular fluid in the white matter, and (*d*) early primary myelin degeneration without damage to axons.

This study was supported by Research Grant National Institute of Health HD-01414-02.

BIBLIOGRAPHY

1. Thomas, L., Aleu, F., Bitensky, M. W., Davidson, M., and Gesner, B., Studies of PPLO Infection. II. The neurotoxin of *Mycoplasma neurolyticum*, *J. Exp. Med.*, 1966, **124**, 1067.

2. Marin, O., and Vial, J. D., Neuropathological and ultrastructural findings in two cases of subacute spongiform encephalopathy, *Acta Neuropath.* 1964, **4**, 218.
3. Nevin, S., McMenemey, W. H., Behram, S., and Jones, D. P., Subacute spongiform encephalopathy, *Brain*, 1960, **83**, 519.
4. Adachi, M., Wallace, B. J., and Wolk, B. W., Ultramicroscopic studies of spongy degeneration, Presented at the Meeting of The American Association of Neuropathologists, Washington, D.C., 1966.
5. Majno, G., and Palade, G. E., Studies on inflammation. I. The effect of histamine and serotonin on vascular permeability, *J. Biophysic. and Biochem. Cytol.*, 1961, **11**, 571.

EXPLANATION OF PLATES

All illustrations are Electron Micrographs.

PLATE 101

FIG. 1. A view from the cortex illustrating the vacuolar nature of the neuropil (*V*) partially surrounding a degenerating glial cell (*DG*). Low power view. × 2800.

FIG. 2. Vacuoles similar to those seen in the preceding figure at a higher magnification demonstrating two adjacent distended glial processes (*GP*) separated from each other by two membranes (arrows). One of the processes contains normal appearing mitochondria (*M*). × 5000.

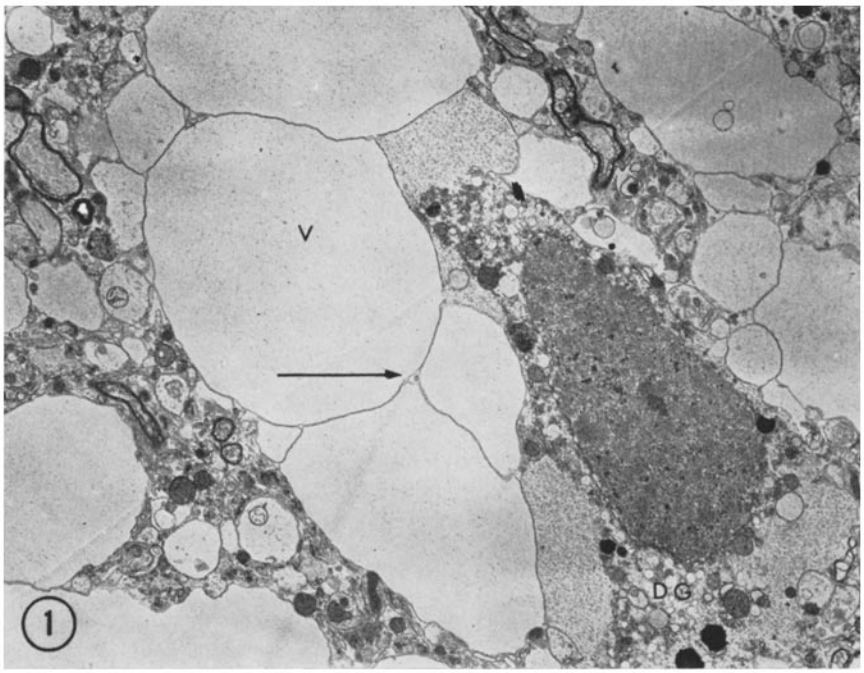

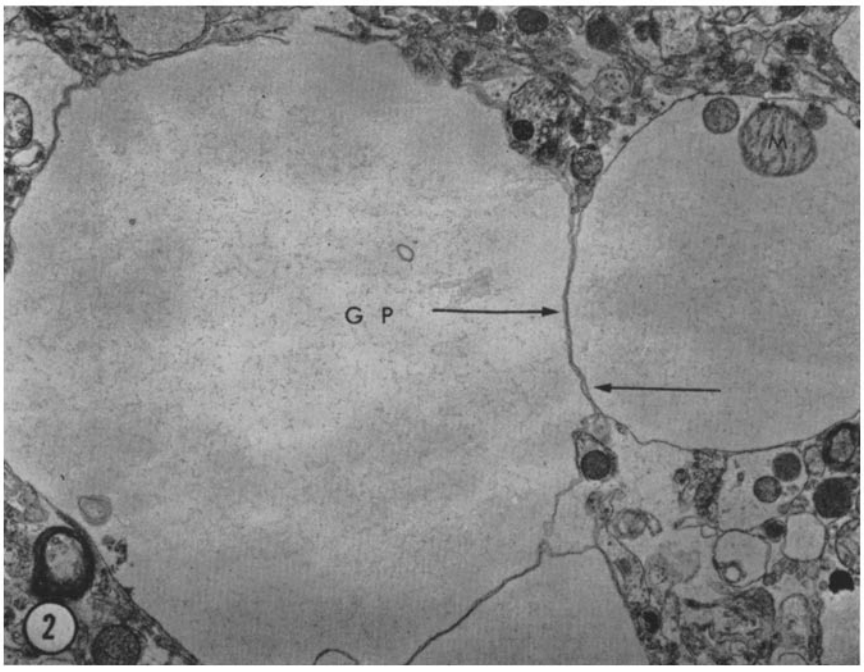

(Aleu and Thomas: Studies of PPLO infection. III)

PLATE 102

FIG. 3. Another large vacuole (*V*) surrounded by compact neuropil (*NP*). The arrow points at the bounding membrane. × 4000.

FIG. 4. Normal glial nucleus adjacent to a distended process (*GP*). The latter is partially surrounded by compact neuropil. The arrow points at the limiting membrane separating the seemingly normal glial cells from the swollen process adjacent to it. × 2800.

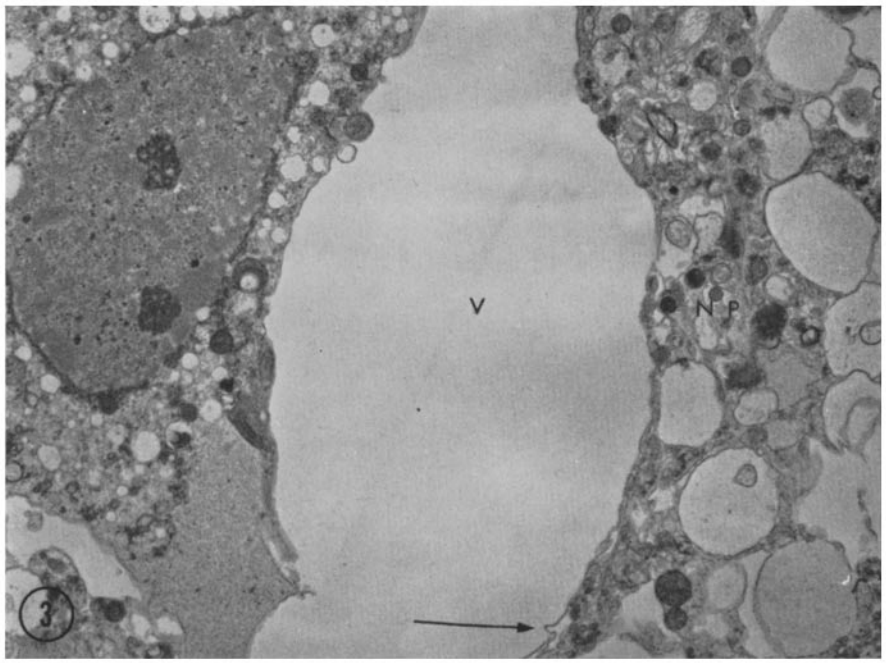

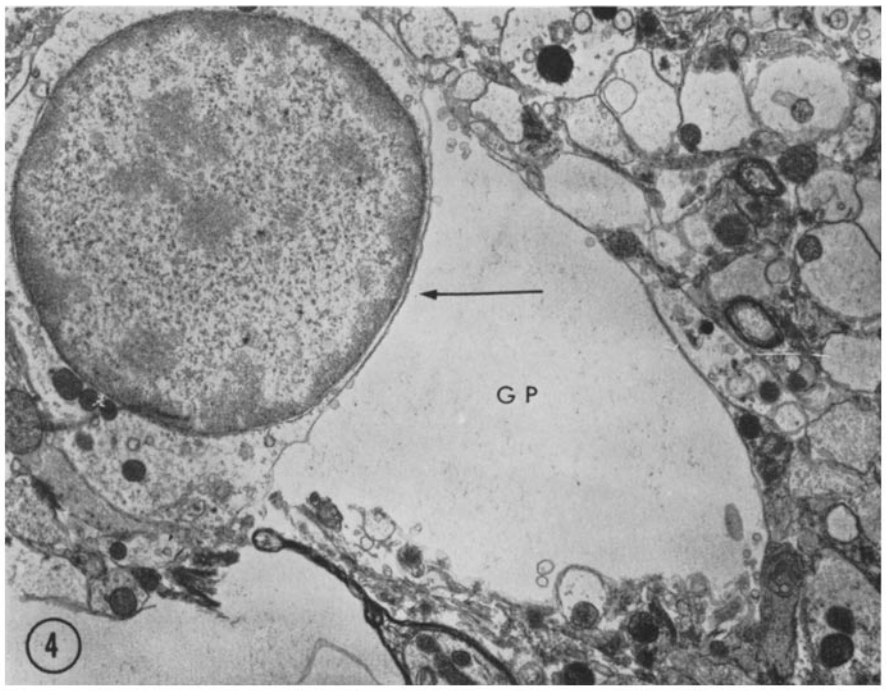

(Aleu and Thomas: Studies of PPLO infection. III)

PLATE 103

FIG. 5. Unidentified cell exhibiting severe degenerative changes which include rhexis of the nuclear membrane (arrow), numerous large vesicles within the cytoplasm, aggregates of lipofuscin (*LG*), autophagic vacuoles (*AV*), and degenerating mitochondria (*M*). × 40,000.

FIG. 6. Active cell seen adjacent to vacuoles with lobular nucleus and dense aggregates of cytoplasmic organelles interpreted as representing a macrophage. The arrows point to a myelin sheath which is partially surrounded by short cytoplasmic extension which may represent an early phagocytic attempt. × 4500.

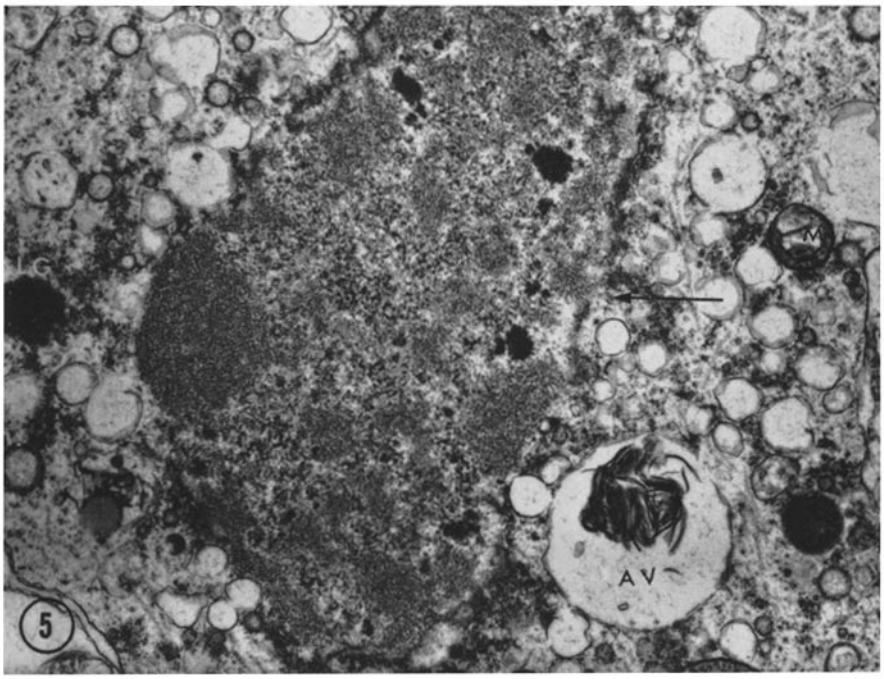

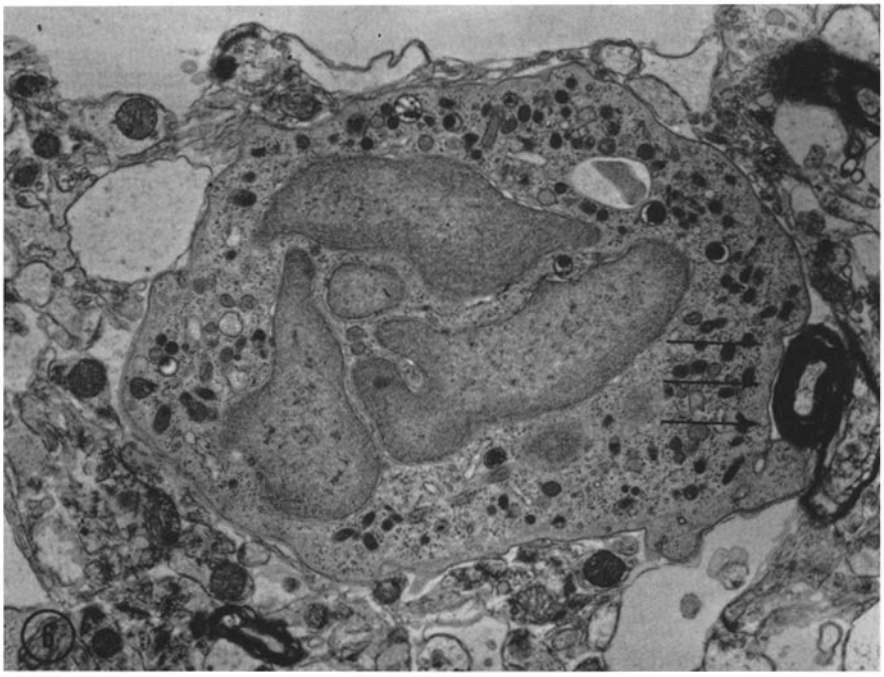

(Aleu and Thomas: Studies of PPLO infection. III)

PLATE 104

FIG. 7. Greatly distended glial process (*PV*) membrane bound (arrows) partially surrounding a small vessel (*C*). The adjacent neuropil (*NP*) includes a number of mildly dilated glial processes but it has a compact appearance. × 4000.

FIG. 8. Portion of a capillary wall, the lumen side is marked (*LU*). Two adjacent endothelial cells are well visualized illustrating the desmosome (*A*) and the 100 A gap which separates both elements (*B*). The basement membrane (*BM*) and neighboring glial process (*AP*) are unremarkable. × 30,000.

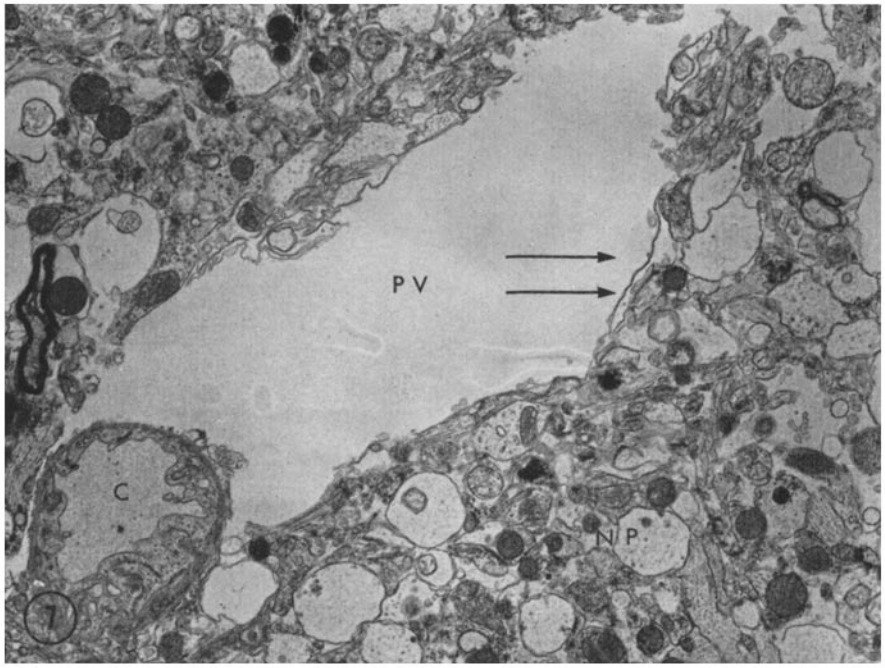

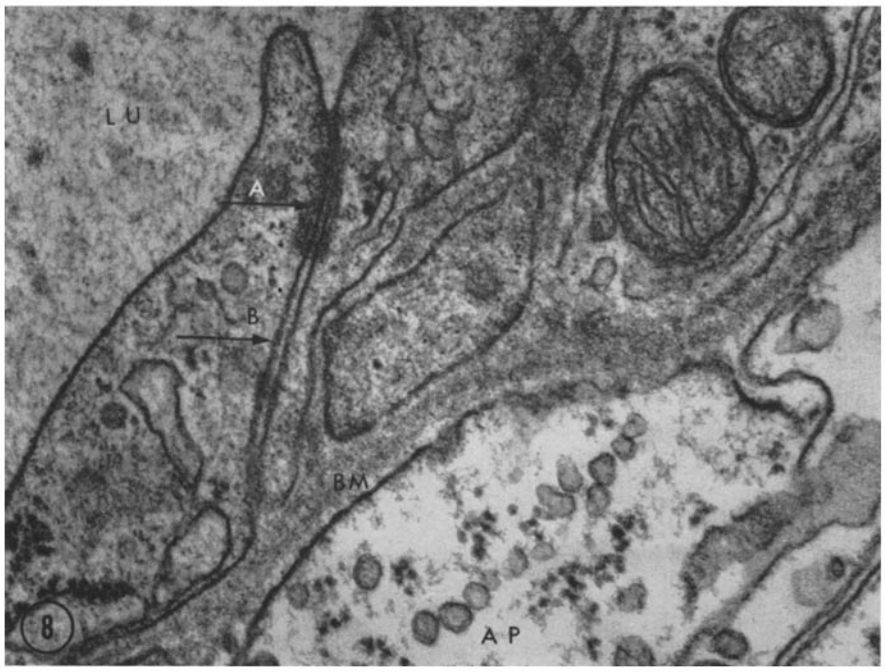

(Aleu and Thomas: Studies of PPLO infection. III)

PLATE 105

FIG. 9. Low magnification view of cortex (*NP*) and white matter. The arrows point at the junction of both. Within the latter large vacuoles (*V*) separating the myelinated axons are also seen. × 3500.

FIG. 10. A view similar to the preceding one illustrating distended glial processes (*GP*) in the neuropil (*NP*), areas of communication of free extracellular space between white matter and cortex (arrows), and increased extracellular space within the white matter (*ES*). × 3500.

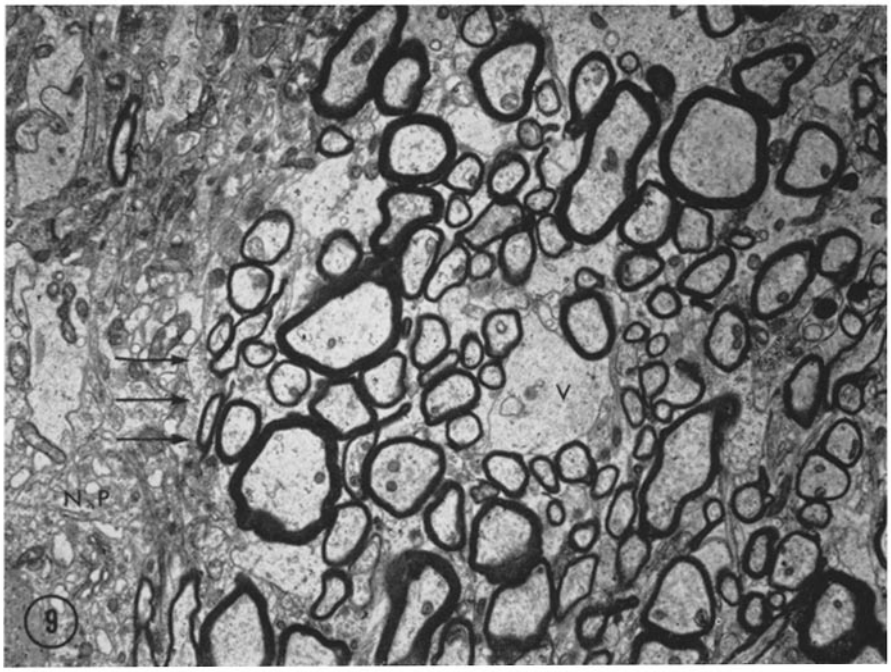

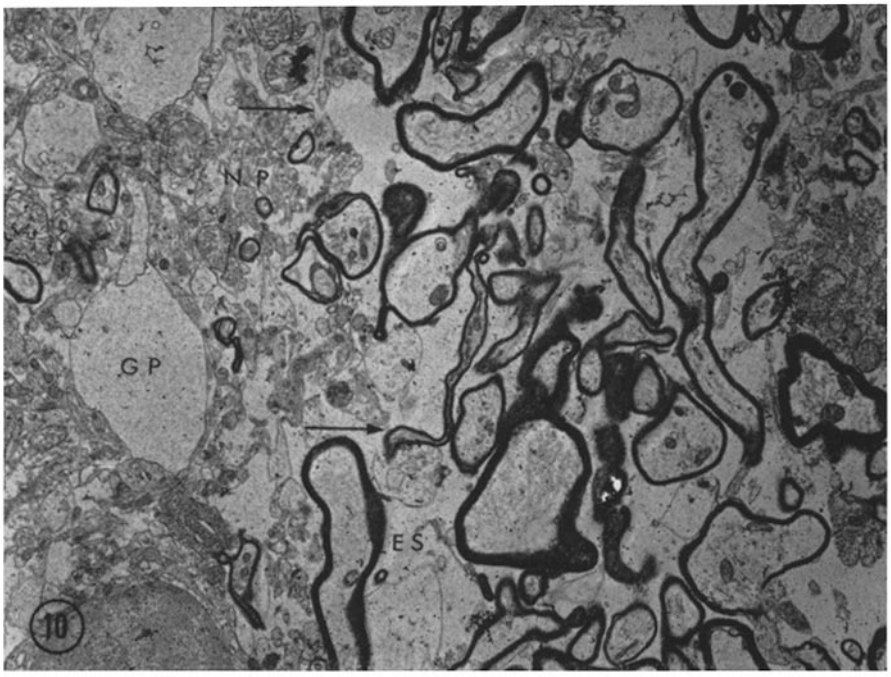

(Aleu and Thomas: Studies of PPLO infection. III)

PLATE 106

FIG. 11. Greatly distended periaxonal spaces (*PAS*) between a normal axon (*A*) and an intact myelin ring were commonly seen. × 7000.

FIG. 12. Distorted myelin ring due to mechanical displacement caused by adjacent distended glial processes. The arrows point to the deformation of the ring. × 10,500.

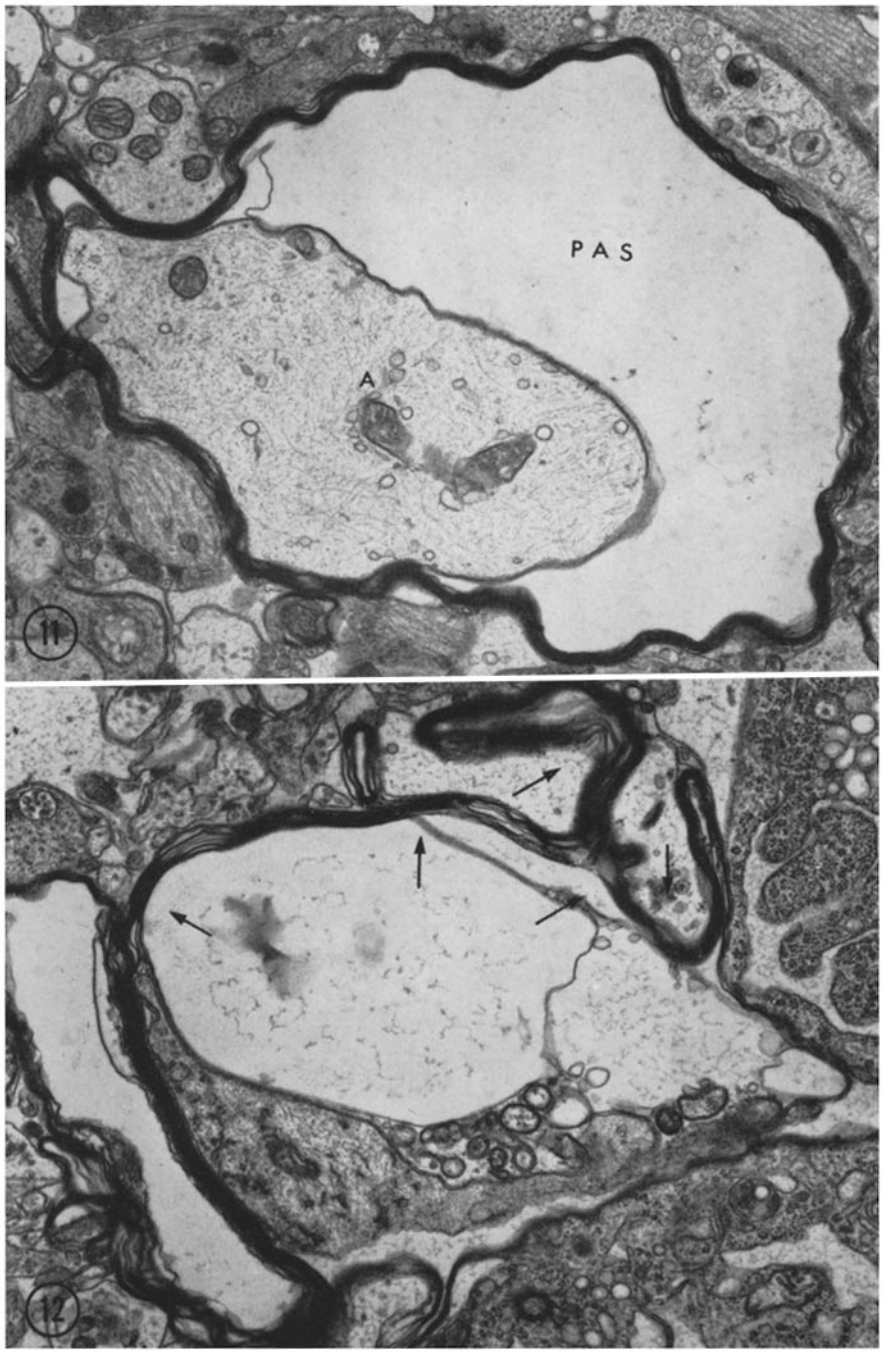

(Aleu and Thomas: Studies of PPLO infection. III)

PLATE 107

FIG. 13. Another example of myelin compression (*CMS*) caused by neighboring swollen cellular processes (*SP*). × 13,500.

FIG. 14. Early myelin degeneration. The axon (*A*) is intact and the axoplasm clear. The surrounding myelin exhibits the formation of a small digestion chamber (*DC*). × 20,000.

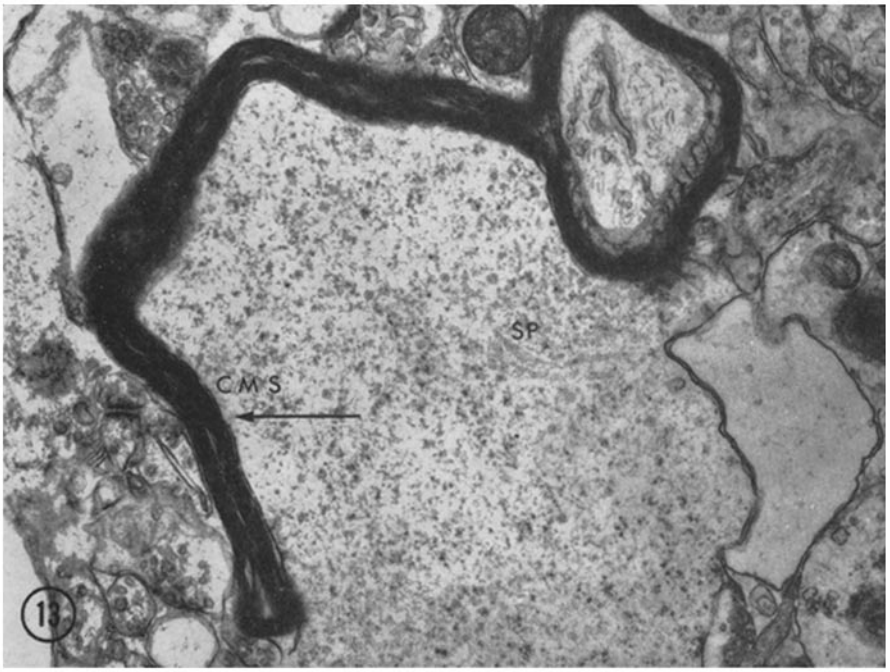

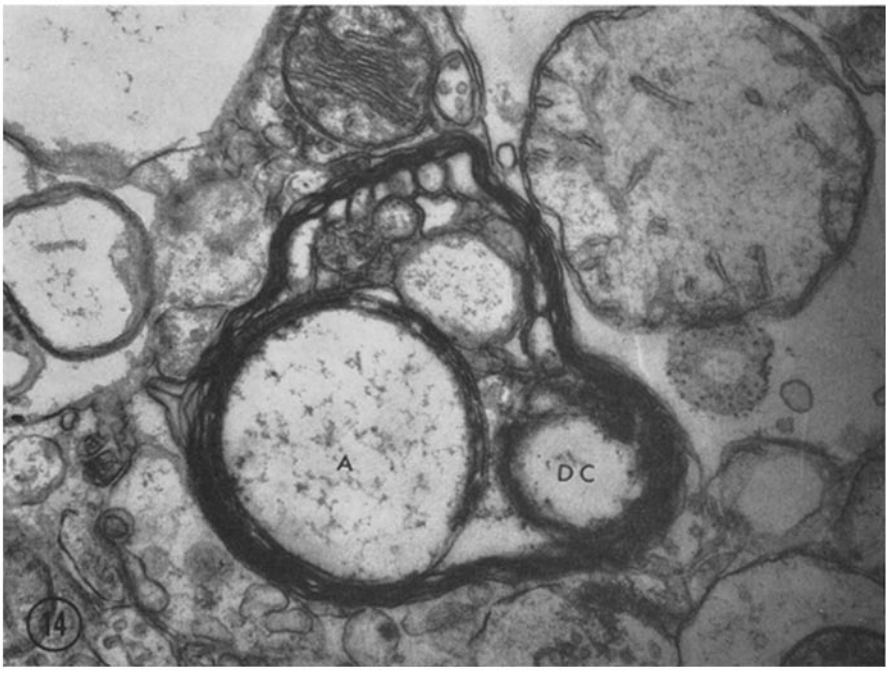

(Aleu and Thomas: Studies of PPLO infection. III)